Strength of vibration-welded polycarbonate–poly(butylene terephthalate)-blend butt welds

Vijay K. Stokes
GE Corporate Research and Development, Schenectady, NY 12301, USA
(Received 13 November 1990; accepted 13 February 1991)

In vibration welding of thermoplastics, frictional work done by vibrating two parts under pressure, along their common interface, is used to generate heat to effect a weld. Previous work characterized the effects of factors such as weld frequency, weld pressure, and weld time on the welding process and weld strength, and showed that the most important factor affecting weld strength of neat resins is the weld penetration—the decrease in the distance between the parts being welded that is caused by lateral outflow of material in the molten film. This paper is concerned with strengths of vibration-welded butt joints of polycarbonate–poly(butylene terephthalate) blends. Weld strengths were mapped at room temperature and at $-29°C$ at strain rates of $0.25 \times 10^{-2}\ s^{-1}$ and $0.25\ s^{-1}$. It was possible to achieve weld strengths equal to that of the base material. Tests on two blends showed that the low-temperature and high-strain-rate strengths and strains at failure can be significantly improved by changing the content of impact modifiers.

(Keywords: welding of thermoplastics; vibration welding; weld strength of PC–PBT blend; low-temperature weld strength; strain-rate effects)

INTRODUCTION

This paper is concerned with the vibration welding of a blend (PC–PBT) of BPA polycarbonate (PC) and poly(butylene terephthalate) (PBT), which inherits its toughness from PC and its chemical resistance from PBT. The complex morphology of this class of blends has been characterized by Hobbs *et al.*[1]. For the last decade, this PC–PBT blend has been the material of choice for making non-reinforced, all-plastics automotive bumpers that can withstand impacts at 8 km h^{-1}. Many of these bumpers have been fabricated by vibration welding of an injection-moulded back plate to an injection-moulded C-section fascia. This study was motivated by the need to establish the strength of the vibration welds in this demanding load-bearing application.

In vibration welding of thermoplastics, frictional work done by vibrating two parts under pressure, along their common interface, is used to generate heat to effect welds[2]. Previous work on vibration welding[2–6] has focused on characterizing the effects of weld factors such as the weld frequency, the amplitude of the vibratory motion, the weld pressure, the weld time, and the part thickness on the process conditions and on the weld strengths of joints of the same material. That work has shown that, under the right conditions, weld strengths equal to that of the base material can be achieved.

The process of vibration welding is known to consist of four phases[2,3], as shown schematically in *Figure 1*. In the first phase, Coulomb friction generates heat at the interface, raising its temperature to the point at which the polymer can undergo viscous flow. In the second phase, the interface begins to melt and the mechanism of heat generation changes from solid Coulomb friction to viscous dissipation in the molten polymer. The molten polymer begins to flow in a lateral direction, resulting in an increase in the weld penetration—the distance by which the parts approach each other as a result of lateral flow. In the third phase, the melting and flow are at steady state, and the weld penetration increases linearly with time. When the machine is shut off, the weld penetration continues to increase because the weld pressure causes the molten film to flow until it solidifies; this is phase IV.

Systematic weld tests on polycarbonate[4], poly(butylene terephthalate), polyetherimide, and modified polyphenylene oxide[5] have shown that the most important parameter controlling the strengths of welds of the same material is the weld penetration. Very high weld strengths—equal to those of the neat resins—can be achieved for penetrations greater than a threshold value.

The purpose of this paper is to evaluate the effects of impact-modifier content and process conditions on the weld strength of PC–PBT.

MATERIALS AND TEST PROCEDURE

To demonstrate the improvement in the low-temperature ductility of PC–PBT blends by the use of impact modifiers, two grades having different amounts of impact modifiers were tested. The materials used were commercially available. The first (XENOY* 1101), which will be referred to as PC–PBT-X, has roughly equal amounts of PC and PBT with 10% impact modifier. The second (XENOY 1102), which will be referred to as PC–PBT, also has about equal amounts of PC and PBT, but contains 15% impact modifier; the impact modifier content was increased to improve the ductility and impact performance of this material, especially at low temperatures. All the test data were obtained from specimens

* XENOY is a registered trademark of General Electric Company

0032-3861/92/061237-07

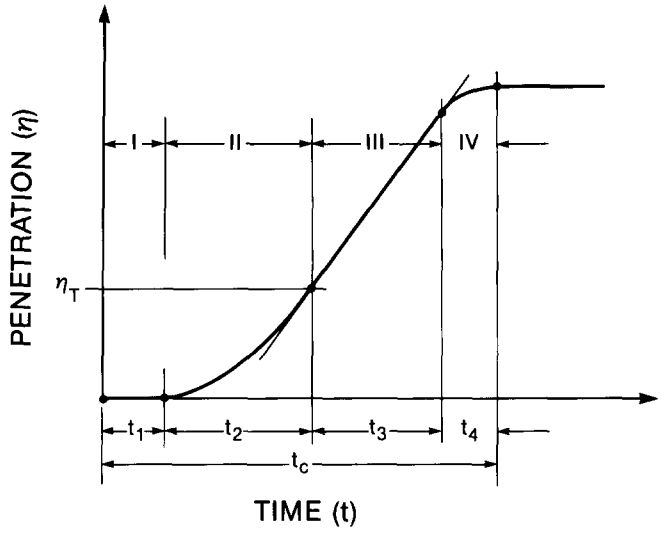

Figure 1 Schematic penetration–time curve showing four phases of the vibration welding process

cut from 6.35 mm thick injection-moulded plaques of PC–PBT-X and PC–PBT. The edges of each specimen were machined to obtain rectangular blocks of size 76.2 × 25.4 × 6.35 mm. Machining the edges of the rectangular specimens made it possible to accurately align two specimens for making a butt weld.

All the welds were performed on a research vibration welding machine[2] on which accurately aligned butt welds can be made under controlled conditions, via an interfacial vibratory motion $z = a\sin(2\pi nt)$, where a is the weld amplitude and n the weld frequency. All the welds were made at a frequency $n = 120$ Hz, at two weld pressures $p_0 = 0.82$ and 1.71 MPa. The amplitude was varied between $a = 0.635$ and 1.65 mm. Because of the automotive bumper applications of this material, the weld strength was tested both at room temperature (22°C) and at −29°C. Strain rate effects were evaluated by conducting the tensile strength tests at nominal strain rates of 0.25×10^{-2} and $0.25\ s^{-1}$.)

Details of the weld procedure were described previously[4]. Two machined specimens are fixed in the upper and lower grips provided on the vibration welding machine. The desired weld frequency and weld amplitude are preset on the servohydraulic control system for generating the interfacial vibratory displacement. The weld surfaces are brought into contact and the desired weld pressure is applied to the interface. During welding, the machine vibrates the interface at amplitude a and frequency n under constant pressure p_0 until the weld penetration equals a preset value η_0. The machine then automatically shuts off after algining the two weld surfaces to their initial position. The weld is allowed to solidify under the same pressure p_0, after which the welded specimen is removed from the grips. The resulting as-welded specimen has nominal dimensions of 152.4 × 25.4 × 6.35 mm. During the welding process, the weld penetration is continuously recorded as a function of time.

Welding tests were terminated at different preset values of weld penetration, which would be the penetration at the end of phase III of the weld process. However, because the weld pressure causes the molten film to flow until it solidifies, the penetration increases by a very small amount after the machine is shut off. As a result, the final penetration at the end of the weld is slightly larger than the preset value η_0. Throughout this paper, penetration data refer to the *final* penetration, η_F, measured at the end of each test.

The welded specimen, of nominal size 152.4 × 25.4 × 6.35 mm, has a continuous 'flash', and hence a continuous weld, except at the ends of the 25.4 mm side (*Figure 2a*). In order to obtain a homogeneous weld specimen, 3.17 mm thick layers are routed out from each end, resulting in a 152.4 × 19 × 6.35 mm rectangular specimen (*Figure 2b*). Finally, this specimen is routed down to the shape of an ASTM D638 tensile test specimen, in which the 50.8 mm gauge length has a cross-section of 12.7 × 6.35 mm (*Figure 2c*). In a tensile test the initial length of the specimen between grips is 101.6 mm.

The tensile bar, which has a uniform transverse butt weld at mid-length, is then subjected to a tensile failure test at constant displacement rate, in which the strain across the weld is monitored with an extensometer. The tensile tests were conducted at two displacement rates: 0.25 and 25 mm s^{-1}. Over a specimen length of 101.6 mm between grips, these displacement rates correspond to *nominal* strain rates of 0.25×10^{-2} and $0.25\ s^{-1}$, respectively. Low-temperature tests were done by enclosing the specimen in a chamber cooled by liquid nitrogen.

As in earlier work[4–6], the weld strength in this study was obtained by dividing the load at failure by the *original* cross-sectional area of the specimen. Because of large local deformations, the true stress at failure would in most cases be larger than the nominal stresses indicated by the data in this paper. Because the weld flash or 'bead' is not removed in most applications, in this study the weld flash was not machined off before a tensile test. There is every reason to believe that, in contrast to metals, the strength of welds with the flash in place is no higher than if the flash had been machined off[4,5].

The average strain across the weld was monitored by a 25.4 mm gauge-length extensometer. As a result, the

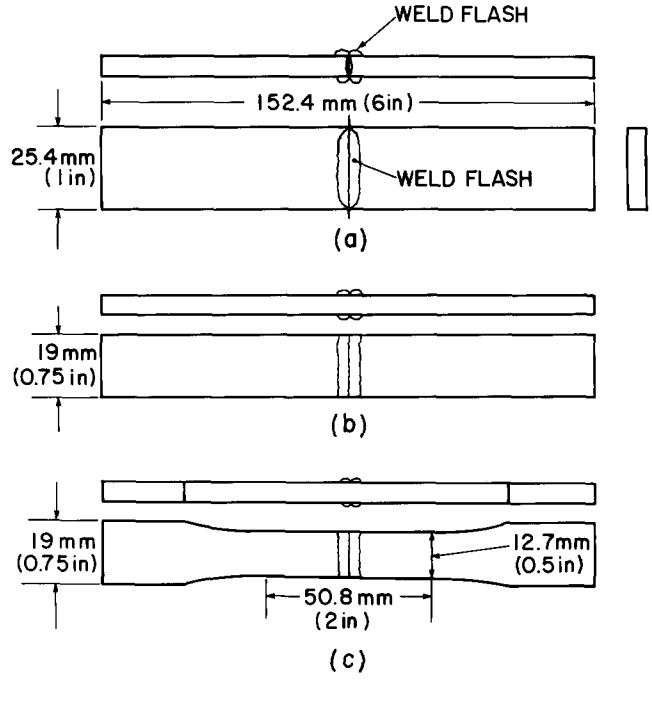

Figure 2 Specimen geometry for determining the strength of butt welds; (a), (b), (c), see text

actual strains would be grossly underestimated once non-homogeneous strain localization sets in. Thus the values of the strains at failure reported in this study should be interpreted with care. These values represent only the lower limits of the strains at failure at welds; the actual strains could be much higher.

RESULTS

Penetration–time data

Figure 3 shows the variation of weld penetration with time for 6.35 mm thick specimens of PC–PBT-X at constant weld frequency and weld pressure for four weld amplitudes. Each of the four curves exhibits the four phases of welding shown in *Figure 1*. In this respect the penetration–time curves are similar to those obtained for several neat resins[2]. In addition, there is evidence that during phase I the penetration can assume small negative values. This can clearly be seen in the curve corresponding to the lowest amplitude (0.64 mm). This phenomenon has been observed by others[7] and can be attributed to thermal expansion at the heated interface. It is important to note that the duration of phase I is a strong function of the weld surface finish and alignment. As a result, the penetration–time curves for tests carried out under identical machine settings can be located in different regions of the time axis, but they can be superimposed by a translation along the time axis. However, the steady-state penetration rate is not sensitive to the initial surface finish and alignment.

The variation of the steady-state penetration rate with the amplitude is shown in *Figure 4*. Although the mean 'friction', or effective, velocity is directly proportional to the weld amplitude, the power absorbed by the weld process is not. Rather, the power absorbed in the steady state is proportional to the product of the effective velocity and the shear stress being imposed on the melt. The shear stress depends on the shear rate (velocity gradient)—which in turn depends on the melt thickness—and the viscosity, which is a strong function of the temperature and the shear rate. These non-linear couplings explain why the steady-state penetration rate in *Figure 4* is not a linear function of the weld amplitude. This also explains why an increment $\Delta a = 0.31$ mm from $a = 0.64$ to 0.95 mm has a much larger effect on the penetration

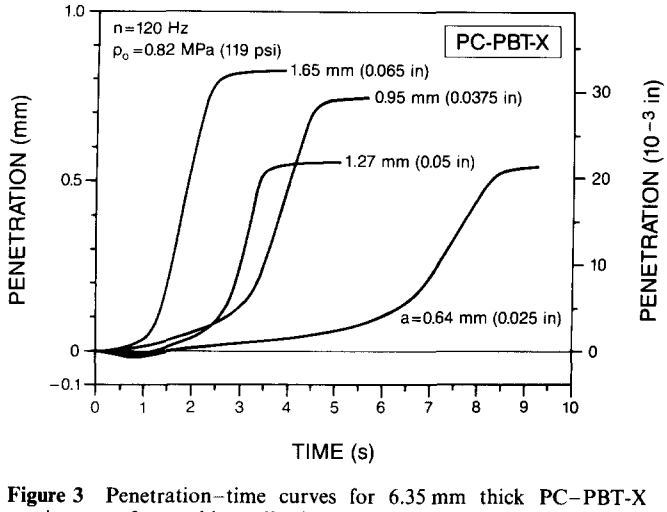

Figure 3 Penetration–time curves for 6.35 mm thick PC–PBT-X specimens at four weld amplitudes ($n = 120$ Hz, $p_0 = 0.82$ MPa)

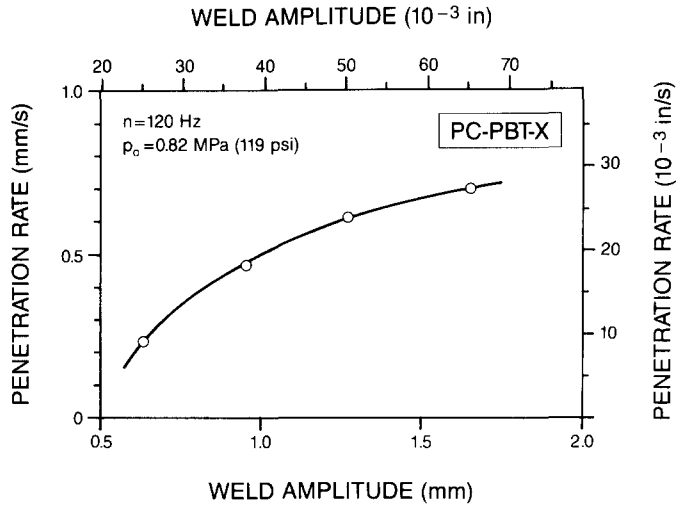

Figure 4 Variation of penetration rate with weld amplitude for 6.35 mm thick PC–PBT-X specimens ($n = 120$ Hz, $p_0 = 0.82$ MPa)

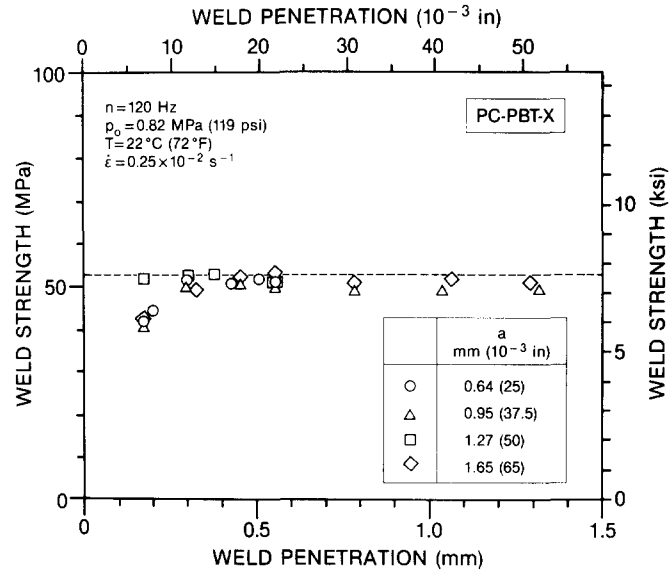

Figure 5 Strength of PC–PBT-X welds at room temperature and $\dot{\varepsilon} = 0.25 \times 10^{-2}\,s^{-1}$ *versus* penetration at four weld amplitudes ($n = 120$ Hz, $p_0 = 0.82$ MPa)

curve than does the same increment from $a = 0.95$ to 1.27 mm (see *Figure 3*). Higher weld pressures result in increased penetration rates, but the increases caused by pressure are relatively much smaller than those caused by increases in weld amplitude.

Strength of PC–PBT-X welds

Figure 5 shows the room-temperature strengths (strain rate $0.25 \times 10^{-2}\,s^{-1}$) of PC–PBT-X butt welds as a function of weld penetration, at one weld pressure for four weld amplitudes. Clearly, weld amplitude does not affect weld strength. Also, for penetrations greater than a threshold of about 0.25 mm, weld strength is not affected by the penetration. For penetrations greater than this threshold, the weld strength essentially equals the neat-resin strength, indicated by the dashed line. This behaviour is similar to that of other neat polymer resins[4,5].

Strength and ductility data for PC–PBT-X welds whose strengths are shown in *Figure 5* are listed in *Table 1*.

In this table η_F is the final penetration after the weld has solidified; t_0 is the time during which the interface is vibrated, i.e. the time at which phase III ends; and σ_w is the measured weld strength based on the original cross-sectional area. The relative weld strength σ_w/σ_u compares the strength of the weld with that of the base resin, σ_u. At a strain rate $\dot{\varepsilon} = 0.25 \times 10^{-2}\ s^{-1}$, several tests resulted in a mean value of $\sigma_u = 53$ MPa. Because of inherent variations in σ_u, values of σ_w/σ_u in the region of 0.98 essentially correspond to welds whose strengths equal that of the base material. For the higher-strength welds, the strains at failure across the welds, as measured by the extensometer, were quite high. The base resin failed after undergoing stable necking at strains well in excess of 5%.

Table 1 includes two additional sets of data, corresponding to high penetrations of $\eta_F = 1.80$ and 2.59 mm, not shown in *Figure 5*. Clearly, high penetrations do not affect the weld strength.

The strengths of PC–PBT-X welds, at a temperature of −29°C and a strain rate of $0.25 \times 10^{-2}\ s^{-1}$, as a function of penetration are shown in *Figure 6*. Here again, strengths equal to that of the base material (dashed line) can be achieved. However, there is more scatter in the data. Although no systematic trend can be discerned from these sparse data, the lowest amplitude ($a = 0.64$ mm) does appear to result in lower weld strength. Note that at this temperature and strain rate, the base resin has a higher strength of $\sigma_u = 68.8$ MPa.

Figure 7 shows the strengths of PC–PBT-X welds, at −29°C but at a higher strain rate of $0.25\ s^{-1}$, *versus* penetration. Clearly, at this higher strain rate, the weld strength is significantly lower than that of the basic resin ($\sigma_u = 78.0$ MPa).

Strength and ductility data for PC–PBT-X welds, tested at −29°C, for the two strain rates of $\dot{\varepsilon} = 0.25 \times 10^{-2}$ and $0.25\ s^{-1}$, are listed in *Table 2*. The strains at failure are somewhat lower at the higher strain rate. Moreover, a comparison with equivalent welds tested at 22°C (*Table 1*) shows that the strains at failure are lower at −29°C. At $\dot{\varepsilon} = 0.25 \times 10^{-2}\ s^{-1}$, a solid specimen of the base resin tested at −29°C failed at a strain of 4.95% just after a neck had begun to form outside the extensometer. At this strain rate, the base resin underwent stable necking at 22°C. A solid specimen of the resin tested at the higher strain rate of $0.25\ s^{-1}$ at −29°C did not fail at the extension cutoff of 12.7 mm, at which the specimen was unloaded. This implies that this specimen had not failed at strains in the region of 10%.

Table 1 Strength and ductility of welds of PC–PBT-X tested at 22°C at a strain rate of $0.25 \times 10^{-2}\ s^{-1}$ ($n = 120$ Hz; $p_0 = 0.82$ MPa)

a (mm)	η_F (mm)	t_0 (s)	σ_w (MPa)	$\frac{\sigma_w}{\sigma_u}$	$100\varepsilon_0$
0.64	0.18	8.00	42.4	0.80	2.4
0.64	0.20	9.89	44.6	0.84	2.9
0.64	0.30	9.37	52.3	0.99	–
0.64	0.43	9.59	50.5	0.95	3.65
0.64	0.56	10.33	51.2	0.97	4.35
0.64	0.51	8.21	52.0	0.98	–
0.95	0.18	3.12	40.7	0.77	–
0.95	0.30	3.31	50.7	0.96	–
0.95	0.46	3.87	50.4	0.95	3.24
0.95	0.56	3.88	50.7	0.96	3.4
0.95	0.79	4.55	49.2	0.93	3.0
0.95	1.04	4.83	49.1	0.93	2.8
0.95	1.32	5.15	49.2	0.93	3.0
1.27	0.18	2.04	51.5	0.97	4.4
1.27	0.30	2.33	52.1	0.98	–
1.27	0.38	2.93	52.5	0.99	3.85
1.27	0.56	2.72	51.1	0.96	3.5
1.65	0.18	1.45	43.0	0.81	–
1.65	0.33	1.63	49.9	0.94	–
1.65	0.46	1.99	52.3	0.99	4.1
1.65	0.56	2.13	53.2	1.01	–
1.65	0.79	2.32	51.2	0.97	4.35
1.65	1.07	3.17	51.6	0.98	4.5
1.65	1.30	3.10	50.9	0.96	4.15
1.65	1.80	3.98	52.3	0.99	3.95
1.65	2.59	5.28	51.7	0.98	1.75

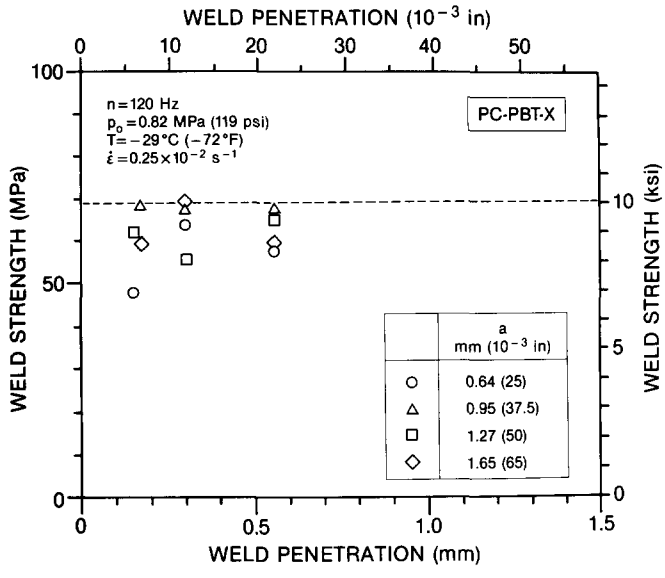

Figure 6 Strength of PC–PBT-X welds at −29°C and $\dot{\varepsilon} = 0.25 \times 10^{-2}\ s^{-1}$ *versus* penetration at four weld amplitudes ($n = 120$ Hz, $p_0 = 0.82$ MPa)

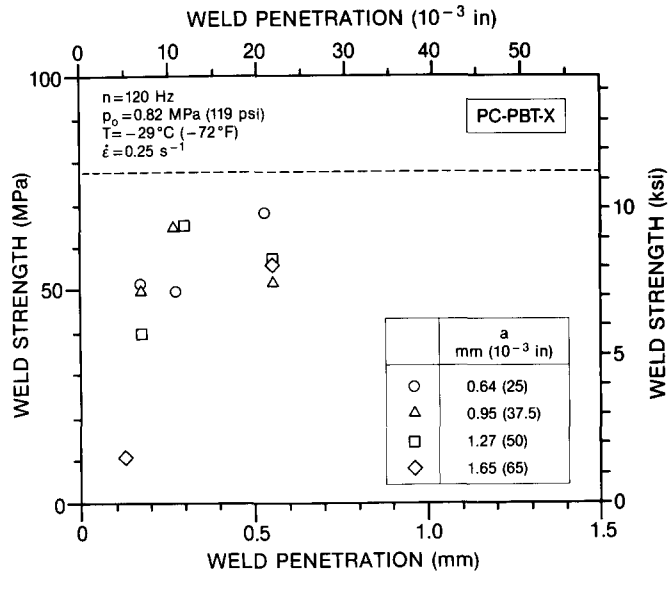

Figure 7 Strength of PC–PBT-X welds at −29°C and $\dot{\varepsilon} = 0.25\ s^{-1}$ *versus* penetration at four weld amplitudes ($n = 120$ Hz, $p_0 = 0.82$ MPa)

Strength of PC–PBT welds

The solid symbols in *Figure 8* show the room-temperature (22°C) weld strengths of PC–PBT butt

Table 2 Strength and ductility of welds of PC–PBT-X tested at −29°C (n = 120 Hz; p_0 = 0.82 MPa)

a (mm)	η_F (mm)	t_0 (s)	$\dot{\varepsilon}$ (10^{-2} s^{-1})	σ_w (MPa)	σ_w/σ_u	$100\varepsilon_0$
0.64	0.15	–	0.25	48.4	0.70	2.3
0.64	0.30	9.78	0.25	64.5	0.94	3.5
0.64	0.56	6.62	0.25	58.4	0.85	2.95
0.64	0.18	–	25	51.6	0.66	2.2
0.64	0.28	5.90	25	50.5	0.65	2.3
0.64	0.53	8.00	25	68.5	0.88	3.67
0.95	0.18	2.64	0.25	68.7	1.00	4.15
0.95	0.30	2.95	0.25	67.7	0.98	4.3
0.95	0.56	4.25	0.25	68.1	0.99	4.2
0.95	0.18	2.23	25	51.0	0.65	2.35
0.95	0.28	2.80	25	65.2	0.84	3.4
0.95	0.56	3.69	25	52.2	0.67	2.4
1.27	0.15	1.65	0.25	62.2	0.90	–
1.27	0.30	1.80	0.25	55.6	0.81	2.65
1.27	0.56	2.48	0.25	64.6	0.94	3.6
1.27	0.18	1.82	25	39.6	0.51	1.72
1.27	0.30	–	25	65.2	0.84	3.4
1.27	0.56	2.16	25	57.4	0.74	2.7
1.65	0.18	1.08	0.25	59.9	0.87	3.13
1.65	0.30	1.23	0.25	69.9	1.02	6.5
1.65	0.56	1.94	0.25	59.9	0.87	3.0
1.65	0.13	0.93	25	11.7	0.15	0.5
1.65	0.56	1.66	25	57.0	0.73	2.7

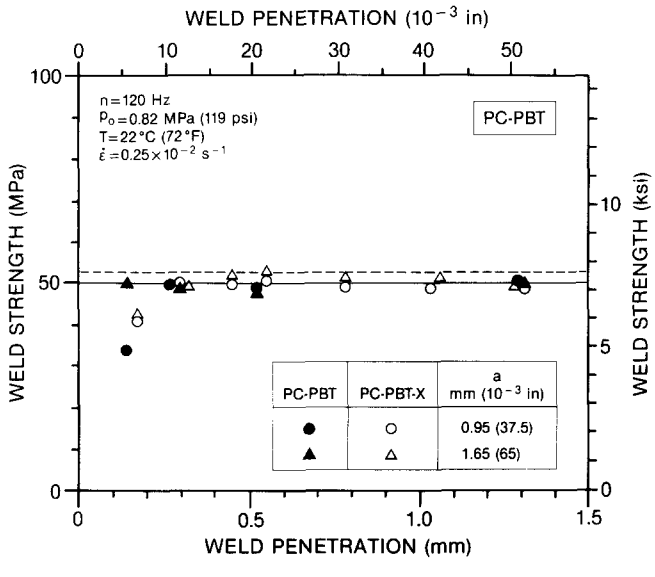

Figure 8 Strength of PC–PBT welds at room temperature and $\dot{\varepsilon}$ = 0.25 × 10^{-2} s^{-1} *versus* penetration at two weld amplitudes (n = 120 Hz, p_0 = 0.82 MPa)

welds as a function of weld penetration for two different amplitudes. The strength of the neat resin is indicated by the solid line. For purposes of comparison, the strengths of PC–PBT-X welds are shown by open symbols, and the strength of neat PC–PBT-X by a dashed line. Clearly, the amplitude does not affect the strength of PC–PBT welds, and the threshold penetration for achieving good welds is about the same as for PC–PBT-X. Based on the data in this figure, the only difference between the two blends would appear to be that PC–PBT has a slightly lower strength (σ_u = 50.1 MPa) than that of PC–PBT-X (53 MPa).

The room-temperature strength of PC–PBT *versus* penetration, at two weld amplitudes and two weld pressures, is shown in *Figure 9*. Clearly, variation of weld pressure in the range 0.82–1.71 MPa does not have any effect on weld strength.

Strength and ductility data for the PC–PBT specimens featured in *Figures 8* and *9* are listed in *Table 3*. A comparison of the final columns of *Tables 3* and *1* shows the significant improvement in the room-temperature failure strains across welds of PC–PBT over those of PC–PBT-X.

Table 3 also contains data for welds made at a pressure of p_0 = 0.31 MPa at two different weld amplitudes; these data are not shown in *Figures 8* and *9*. While the weld strengths at this low weld pressure are only marginally smaller than the strengths at higher pressures, the strains at failure are significantly lower.

The strength of PC–PBT welds at −29°C, at the higher strain rate of $\dot{\varepsilon}$ = 0.25 s^{-1}, as a function of weld

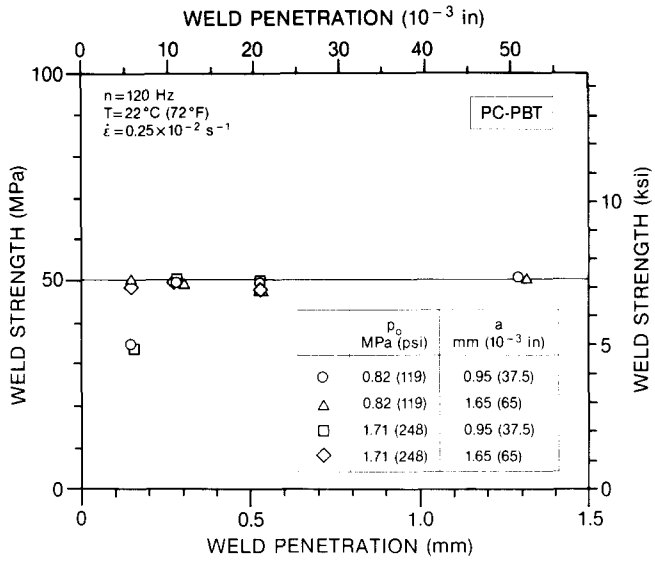

Figure 9 Strength of PC–PBT welds at room temperature and $\dot{\varepsilon}$ = 0.25 × 10^{-2} s^{-1} *versus* penetration at four weld amplitudes and pressures (n = 120 Hz)

Table 3 Strength and ductility of welds of PC–PBT tested at 22°C at a strain rate of 0.25 × 10^{-2} s^{-1} (n = 120 Hz)

a (mm)	p_0 (MPa)	η_F (mm)	t_0 (s)	σ_w (MPa)	σ_w/σ_u	$100\varepsilon_0$
0.95	0.31	0.33	7.9	47.2	0.94	4.26
0.95	0.31	0.53	6.8	48.9	0.98	7.75
0.95	0.82	0.15	2.46	34.7	0.69	1.8
0.95	0.82	0.28	2.74	50.4	1.01	10.8
0.95	0.82	0.53	3.14	49.2	0.98	8.0
0.95	0.82	1.30	4.53	51.4	1.03	19.1
0.95	0.82	2.54	6.70	50.3	1.01	13.6
0.95	1.71	0.15	1.33	34.1	0.68	2.02
0.95	1.71	0.28	1.65	50.1	1.00	5.85
0.95	1.71	0.53	1.99	50.3	1.00	7.2
1.65	0.31	0.18	3.26	42.5	0.85	3.16
1.65	0.31	0.28	3.35	46.0	0.92	3.02
1.65	0.31	0.56	3.72	48.7	0.97	3.5
1.65	0.82	0.15	1.50	50.5	1.01	9.6
1.65	0.82	0.30	1.79	49.7	0.99	11.5
1.65	0.82	0.53	1.85	48.7	0.97	10.3
1.65	0.82	1.32	3.22	50.5	1.01	5.7
1.65	0.82	2.59	4.73	50.5	1.01	6.34
1.65	1.71	0.15	0.67	50.3	1.01	10.6
1.65	1.71	0.28	0.76	50.4	1.01	11.6
1.65	1.71	0.53	1.26	50.1	1.00	15.5

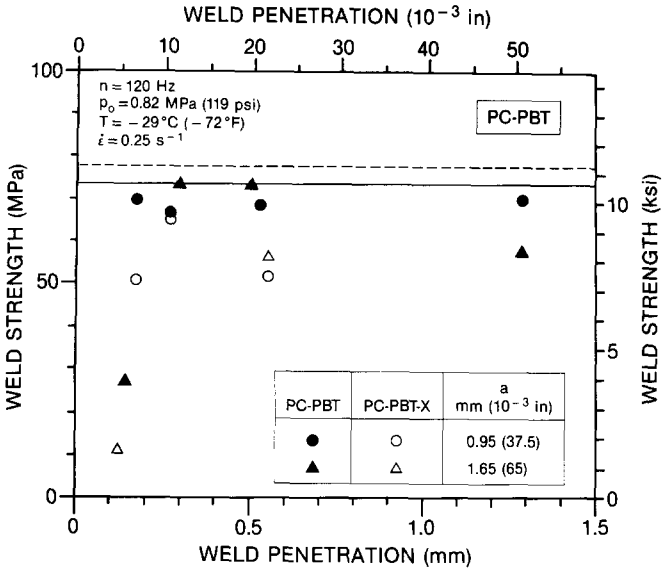

Figure 10 Strength of PC–PBT welds at −29°C and $\dot{\varepsilon} = 0.25\ s^{-1}$ *versus* penetration at two weld amplitudes (n = 120 Hz, p_0 = 0.82 MPa)

Table 4 Strength and ductility of welds of PC–PBT tested at −29°C at a strain rate of 0.25 s^{-1} (n = 120 Hz; p_0 = 0.82 MPa)

a (mm)	η_F (mm)	t_0 (s)	σ_w (MPa)	$\frac{\sigma_w}{\sigma_u}$	$100\,\varepsilon_0$
0.95	0.18	2.36	69.8	0.95	4.5
0.95	0.28	2.70	67.1	0.91	4.15
0.95	0.53	3.16	68.9	0.94	4.1
0.95	1.30	5.15	70.5	0.96	4.4
0.95	2.57	7.33	73.2	1.00	12.5
1.65	0.15	1.47	27.4	0.37	1.2
1.65	0.30	2.09	73.6	1.00	9.6
1.65	0.51	2.20	73.5	1.00	6.85
1.65	1.30	3.09	58.0	0.79	2.89
1.65	2.57	5.21	47.8	0.65	2.16

penetration, is shown in *Figure 10* for two different weld penetrations. The solid line indicates the strength of the neat PC–PBT resin (σ_u = 73.6 MPa) under these test conditions. Data for PC–PBT-X weld strength are shown by open symbols, and the strength of the neat resin by a dashed line (σ_u = 78.0 MPa). Clearly, the strengths of PC–PBT welds are much closer to the strength of the neat resin than in the case of PC–PBT-X welds. Strength and ductility data for these PC–PBT welds are given in *Table 4*.

Not only is the low-temperature strength of PC–PBT at the relatively high strain rate of 0.25 s^{-1} as high as that of the neat resin, the failure strains across the welds are also high. This can be seen by comparing the final columns in *Tables 4* and *3*.

Thus, from the viewpoint of welding, the PC–PBT blend is superior to the PC–PBT-X blend.

Morphology of weld fracture surface

This section is concerned with the effects of weld penetration on the fracture surface. *Figure 11* shows the fracture surface of a PC–PBT-X weld, that was welded at p_0 = 0.82 MPa and a = 1.65 mm to a penetration of η_F = 0.18 mm. The weld was tested to failure at room temperature, at a nominal strain rate of 0.25 × 10^{-2} s^{-1}. This weld failed at a relative weld strength of σ_w/σ_u = 0.81, which is quite high. The weld surface is relatively smooth, indicating that most of the failure occurred in the weld plane.

Figure 12 shows the fracture surface of a PC–PBT-X weld, welded and tested under the same conditions as the

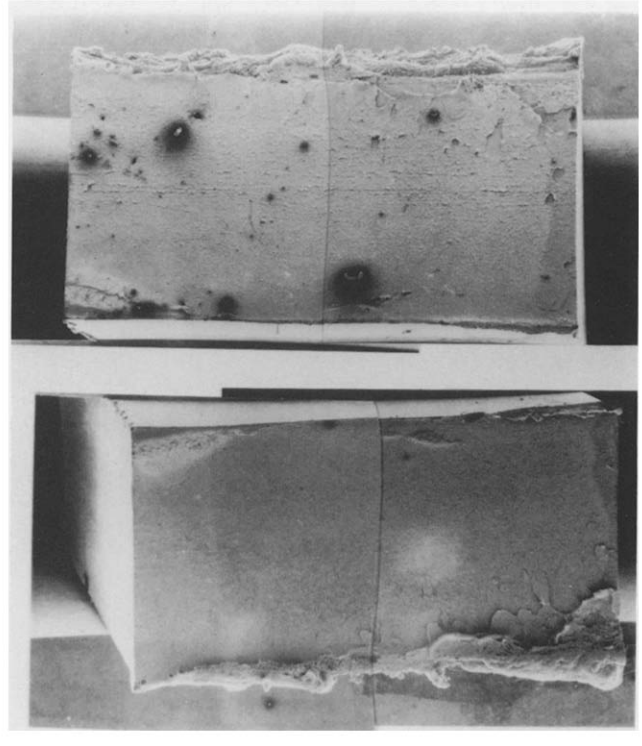

Figure 11 Fracture surface of a 120 Hz PC–PBT-X weld, welded at p_0 = 0.82 MPa and a = 1.65 mm to η_F = 0.18 mm, tested at room temperature at $\dot{\varepsilon} = 0.25 \times 10^{-2}\ s^{-1}$

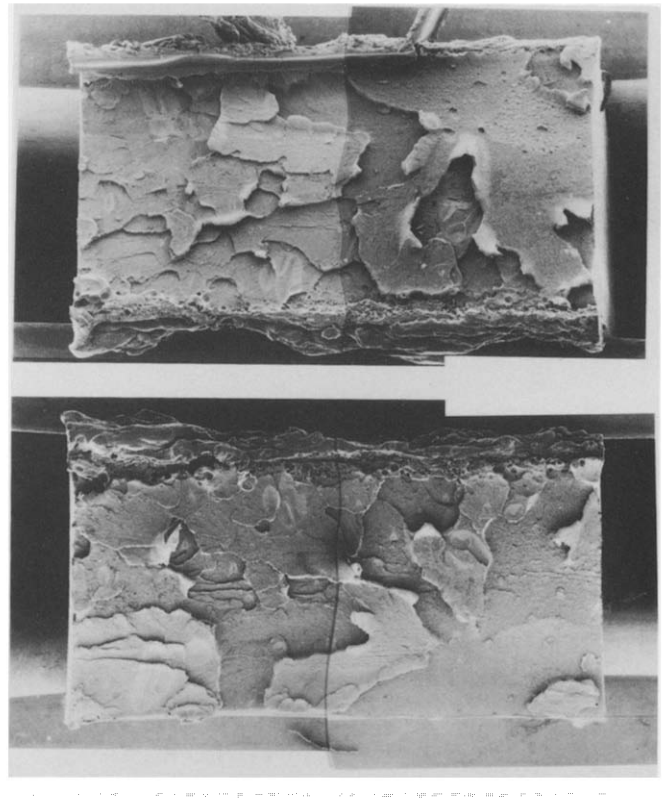

Figure 12 Fracture surface of a 120 Hz PC–PBT-X weld, welded at p_0 = 0.82 MPa and a = 1.65 mm to η_F = 0.33 mm, tested at room temperature at $\dot{\varepsilon} = 0.25 \times 10^{-2}\ s^{-1}$

specimen in *Figure 11*, except that the final penetration was higher ($\eta_F = 0.33$ mm). This weld failed at a higher strength $\sigma_w/\sigma_u = 0.94$. Notice the dramatic change in the fracture surface. The failure is non-planar. Clearly, failure is initiated at many sites within a relatively thick layer of material surrounding the weld interface, and the material undergoes a significant amount of ductile drawing before failure.

The fracture surface for a higher value of $\eta_F = 0.56$ mm, all the other conditions being the same as for the specimens in *Figures 11* and *12*, is similar to that shown in *Figure 12*. This supports the observation that the quality of welds is independent of the penetration for penetrations above a threshold value that corresponds (nominally) to the penetration when the weld process attains a steady state at the beginning of phase III.

CONCLUSIONS

Just as in neat resins[3,4], it has been shown that both the PC–PBT-X and PC–PBT blends weld well; weld strengths equal to that of the neat resin can be achieved under the right conditions. For 120 Hz welds, PC–PBT appears to be particularly insensitive to the weld amplitude. Also within the narrow range of weld pressures used ($p_0 = 0.82$–1.71 MPa), the weld strength is not sensitive to the pressure. (PC–PBT has been shown to have high weld strengths at $p_0 = 0.31$ MPa.) Instead, as with other resins[4,5], the weld strength is controlled by a threshold penetration. Above this threshold the strength is independent of the weld parameters; below this the strength falls off.

For both PC–PBT-X and PC–PBT, the strains at failure across welds are lower at lower temperatures and at higher strain rates, indicating a decrease in ductility. However, this is consistent with the behaviour of these two resins.

While high weld strengths can be achieved in both resins in room-temperature tests (22°C) at low strain rates ($0.25 \times 10^{-2}\ s^{-1}$), the low-temperature (−29°C) high-strain-rate ($0.25\ s^{-1}$) performance of PC–PBT welds is significantly better than that of PC–PBT-X welds: both the strengths and the strains at failure in welds are much closer to the values for the resin for PC–PBT than is the case for PC–PBT-X. Clearly, from the viewpoint of welding, the PC–PBT blend is superior to the PC–PBT-X blend. The increased impact modifier content in PC–PBT, however, does result in a slightly lower strength of the resin (50.1 MPa) compared with that of PC–PBT-X (53 MPa).

ACKNOWLEDGEMENTS

Support provided by GE Plastics is gratefully acknowledged. All the weld and strength tests were carried out by L. P. Inzinna; his enthusiasm and his contributions are greatly appreciated. Special thanks are due to Julia A. Kinloch for her help and patience during the preparation of this paper.

REFERENCES

1 Hobbs, S. Y., Dekkers, M. E. J. and Watkins, V. H. *J. Mater. Sci.* 1988, **23**, 1219
2 Stokes, V. K. *Polym. Eng. Sci.* 1988, **28**, 718
3 Stokes, V. K. *Polym. Eng. Sci.* 1988, **28**, 728
4 Stokes, V. K. *Polym. Eng. Sci.* 1988, **28**, 989
5 Stokes, V. K. *Polym. Eng. Sci.* 1988, **28**, 998
6 Stokes, V. K. *Polym. Eng. Sci.* 1989, **29**, 1683
7 Potente, H. and Kaiser, H. *Polym. Eng. Sci.* 1989, **29**, 1661